Energy and Climate Management, 2026, 2(4): 9400044
https://doi.org/10.26599/ECM.2026.9400044

Article

Total capacity and spatial distribution of wind and solar power in China under the 2035 Nationally Determined Contribution

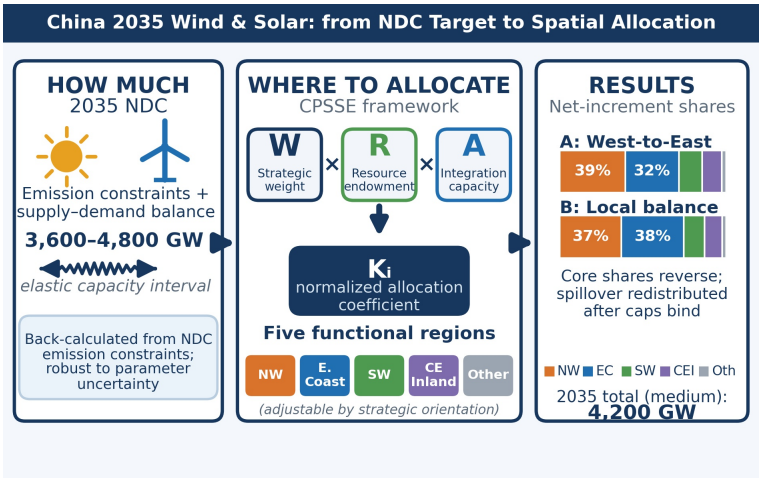
Xueting Li[1,✉], Bin Cai[1], Yusheng Xue[1], Feng Xue[1], Baoguo Shan[2], Qingchen Chao[3], Peipei You[2], Yang Wang[3]

[1]*State Grid Electric Power Research Institute (NARI Group Corporation), Nanjing 211106, China*
[2]*State Grid Energy Research Institute Co., Ltd., Beijing 102209, China*
[3]*National Climate Center, Beijing 100081, China*

Received: 17 August 2026; Revised: 3 September 2026; Accepted: 21 October 2026

© The Author(s) 2026. This is an open access article under the terms of the Creative Commons Attribution 4.0 International License (CC BY 4.0, http://creativecommons.org/licenses/by/4.0/).

ABSTRACT



Against the backdrop of global carbon neutrality, the development targets and spatial distribution of renewable capacity such as wind and solar power are key to achieving the goals of the Nationally Determined Contribution (NDC). China's 2035 NDC target specifies that wind and solar installed capacity should strive to reach 3,600 GW, but its spatial distribution involves multiple coupled constraints—resource endowment, integration space, and energy security—and is a typical cross-domain complex decision-making problem spanning the physical and social systems. Within the cyber-physical-social system in energy (CPSSE) framework, this paper proposes a total-capacity and spatial-allocation method adaptable to different strategic orientations. At the aggregate level, the installed-capacity elastic interval is derived through the coordinated use of NDC emission constraints and the electricity supply–demand framework. At the spatial level, a "strategic weight–resource endowment–integration capacity" three-dimensional correction model is constructed, and regional division is performed based on the cross-domain coupling of the physical and social dimensions. At the engineering level, a truncation-and-redistribution algorithm is introduced to correct the theoretical allocation results under hard constraints. The case results show that the allocation coefficients of the core regions reverse under different strategic orientations and that, after being constrained by physical upper limits, the spillover increment is redistributed to other regions. The method provides a reusable quantitative decision-support tool for medium- and long-term energy planning.

Implications for Energy and Climate Management

Who: National and provincial energy-planning authorities, grid companies, and renewable developers responsible for translating the 2035 NDC target into provincial capacity quotas and project locations.

Management challenge: National targets do not indicate where capacity can actually be built; planners must reconcile strategic priorities with resource endowment, transmission capacity, and land- and sea-use limits, often without a transparent basis for comparing alternatives.

Management implication: Presenting 3,600–4,800 GW as an elastic interval and making the strategic orientation explicit gives decision-makers a reproducible way to compare plans, see which regional limits bind, and anticipate where spillover capacity will land.

KEYWORDS

Nationally Determined Contribution, variable renewable energy, spatial allocation, energy security, capacity planning.

1 Introduction

The global carbon neutrality process is accelerating; however, the IPCC Sixth Assessment Report (AR6) indicates that the sum of existing Nationally Determined Contribution (NDC) commitments still deviates substantially from the 1.5 °C temperature pathway, leaving a significant implementation gap[1]. As the world's largest emitter of greenhouse gases and the largest installer of renewable energy capacity, China's energy transition pathway is critical to achieving the temperature goals of the Paris Agreement. In September 2025, China officially announced its 2035 NDC target, specifying key indicators such as striving for 3,600 GW of wind and solar installed capacity; in 2026, a 3.8% reduction in carbon emissions per unit of gross domestic product (GDP) was further established as a binding indicator, marking the deepening of a phase of dual control over both emission intensity and total emissions.

✉Address correspondence to Xueting Li, lixueting@sgepri.sgcc.com.cn

This target defines the aggregate boundary of wind and solar capacity, yet its spatial distribution must still balance multiple constraints, including resource endowment, potential integration space, and strategic orientation. The large-scale integration of such variable renewable capacity will increasingly challenge the economics of coal-fired power and the flexibility of the power system, a central concern in China's low-carbon power transition[2]. These constraints derive not only from physical conditions such as resources and the power grid but also from governance needs such as regional development and energy security; they are mutually coupled and interdependent, making spatial distribution a typical cross-domain complex decision-making problem. This problem is not unique to China—developing countries such as Indonesia, India, and Vietnam face the common challenge of effectively matching spatial distribution to aggregate targets[3]—and there is an urgent need for reusable quantitative tools for spatial distribution.

Regarding aggregate capacity targets, early studies mostly focused on projections toward 2030[4,5], while recent research has turned to 2035 and longer time horizons[6,7]. Regarding spatial distribution, existing methods mainly include coefficient-weighting approaches[8,9], mathematical programming[10,11], geographic information system (GIS)-based spatial analysis[12,13], and system dynamics[14,15]. Coefficient-weighting approaches can quantify non-economic factors such as national strategy as weights and are suitable for policy-oriented medium- and long-term planning; mathematical programming pursues economic optimality but relies heavily on accurate cost data; GIS-based approaches are suitable for micro-siting and making ecological constraints explicit; and system dynamics is suitable for studying the long-term evolution of socio-technical system transitions. Because this paper focuses on generating distribution plans under several possible strategic orientations, it adopts the coefficient-weighting approach to reduce dependence on accurate cost data and future technical parameters. In parallel, research on spatial patterns under high shares of renewable energy has shown new directions: Ref. [16] conducted a spatial optimization of a European power system with a high share of renewables based on the PyPSA framework, providing a transferable quantitative tool for cross-regional spatial optimization; Ref. [17] proposed that the new power system should build large clean energy bases and distributed renewable energy according to local conditions; and Ref. [18] further proposed a new strategy for energy development that combines "from afar" with "from nearby", reflecting an evolving spatial pattern of simultaneous centralized development with inter-regional transmission and local development with local integration.

Existing studies have made significant progress in resource assessment, aggregate projection, and spatial distribution methods, but three deficiencies remain. First, aggregate targets are mostly single-value projections and have not systematically derived the upper and lower bounds of the installed-capacity interval from NDC emission constraints. Second, existing zoning methods are mostly oriented toward resource endowment or geographic macro-regions and insufficiently account for the coupled physical and social constraints. Third, although new ideas such as combining "from afar" and "from nearby" have been proposed, existing quantitative spatial distribution methods still implicitly assume the one-way "West-to-East power transmission" pattern and cannot reflect the possible two-way power flow under a high share of renewables. There is therefore an urgent need to construct a spatial distribution method that coordinates multiple factors and adapts to multiple strategic orientations.

In essence, the above problem is a complex decision-making issue in which the physical and social dimensions are deeply coupled and supported by information means. Energy transition research involves not only natural science fields such as energy technology and climate science but also social science fields such as energy economics, policy mechanisms, and human behavior; it is a typical cyber-physical-social system in energy (CPSSE) problem[19]. With the large-scale integration of highly uncertain renewable generation and new forms of electricity use, the power system must shift from a beneficiary of the energy transition to an active enabler, and its research framework has correspondingly expanded from the cyber-physical system (CPS) to a CPSSE that encompasses market, policy, and regulatory elements[20], emphasizing the interaction of energy, information, emission, economic, and behavioral flows. The CPSSE framework guides this study as follows: the wind and solar capacity and its spatial distribution cannot consider only physical-dimension factors such as resource endowment, grid constraints, and integration conditions but must also incorporate social-dimension factors such as national strategy, regional development, and energy security, and, through the information dimension's chain of data collection, knowledge extraction, and decision support, translate multiple constraints into quantifiable research results.

This paper focuses on the core link of wind and solar spatial distribution and defines its research boundary as follows: under the constraint of the NDC target, it analyzes possible plans for the total capacity and spatial allocation of wind and solar power in China in 2035. Details of grid engineering planning and operation optimization (such as grid topology design, transmission line construction sequencing, dispatch and operation strategies, and dynamic optimization of transmission-channel utilization), power market conditions, and energy-system economics are not discussed here; the paper uses only the grid transmission capacity ceiling and the load-increment-based integration space as hard boundary conditions for regional allocation, focuses on the 2035 target year, and does not study year-by-year implementation pathways. Within the CPSSE framework, this paper proposes a method for aggregate targets and spatial allocation that is suitable for different strategic orientations. At the aggregate level, it designs an elastic-interval derivation method that back-calculates from NDC emission constraints, enhancing robustness under medium- and long-term uncertainty. At the spatial level, it constructs a "strategic weight–resource endowment–integration capacity" three-dimensional correction model that explicitly quantifies factors such as national strategy and builds the regional division criteria by focusing on the physical and social dimensions, clarifying the functional positioning and boundaries of each region. At the engineering level, it introduces a truncation-and-redistribution algorithm as a constraint-correction mechanism to prevent theoretical allocations from deviating from engineering reality. The interactions between the physical dimension (resource endowment, grid constraints, integration conditions) and the social dimension (national strategy, regional development, energy security) are explicitly quantified through the three-dimensional correction model; the information dimension runs through the method design as a chain of data collection, knowledge extraction, and decision support and is not elaborated separately. Through flexible setting of strategic weights, the method can quantify the new idea of combining "from afar" and "from nearby" into comparable distribution plans, explicitly characterizing the two-way flow trend of simultaneous centralized transmission and local integration under a high share of renewables. The method is country-agnostic and can be generalized to other developing countries facing the challenge of NDC spatial distribution.

2 Methods

2.1 Problem definition and method adaptability

This study focuses on the following question: under the constraint of the 2035 NDC target, what total wind and solar capacity should China reach, and how should this capacity be allocated among regions? This problem involves cross-domain interactions among information, physical, and social systems and exhibits three characteristics. First, multiple constraints are intertwined: constraints such as resource endowment and integration conditions (physical dimension), and energy security and national strategy (social dimension), are coupled with one another. Second, strategic orientations are diverse, and different strategic orientations significantly affect the spatial distribution results. Third, medium- and long-term uncertainty is prominent: facing the 2035 target year, key parameters such as technology costs and electricity load are subject to considerable projection uncertainty.

To address these characteristics, this paper proposes a total-capacity and spatial-allocation method suitable for different strategic orientations. Within the CPSSE framework, the multi-dimensional constraints of information, physics, and society are explicitly quantified through a three-dimensional correction model; the strategic weight coefficients can be flexibly adjusted to rapidly generate differentiated distribution plans; and the aggregate target is back-calculated from NDC emission constraints to determine the upper and lower bounds, enhancing robustness under strategic uncertainty.

2.2 Quantitative analysis workflow of total capacity and spatial distribution

This paper decomposes the core problem into two sub-questions—"how much to grow" and "where to allocate"—and designs a four-step quantitative analysis workflow to answer them in sequence. Step 1, aggregate target derivation: decompose the NDC economy-wide net greenhouse gas (GHG) emission constraint down to the power sector and derive the elastic interval of wind and solar capacity under different reduction intensities, answering "how much to grow". Step 2, regional division: departing from the single-dimensional division based on geographic macro-regions or resource endowment, and comprehensively considering resource endowment and grid constraints (physical dimension) as well as regional development status and national strategy (social dimension), divide the whole country into several functional regions. Step 3, spatial allocation: construct a "strategic weight–resource endowment–integration capacity" three-dimensional correction model to decompose the aggregate target among functional regions. Step 4, regional wind–solar ratio determination: based on regional resource characteristics, technology progress trends, and system constraints, determine the appropriate photovoltaic (PV)-to-wind ratio in 2035. Among these, Steps 2–4 unfold progressively along "zoning–allocation–ratio" and jointly answer "where to allocate". Within the CPSSE framework, the constraints of the physical and social dimensions are explicitly incorporated through the regional division criteria and the three-dimensional correction model, and the information dimension runs through the method design as a chain of data collection–knowledge extraction–decision support. Specifically, data collection corresponds to the data sources in Section 3.1, knowledge extraction draws on the methods in Section 2 and the case study in Section 3, and decision support is embodied in the discussion in Section 3.6, ensuring that the multiple constraints are treated consistently within the same analytical framework. The overall workflow is illustrated in Figure 1.

2.3 Aggregate target derivation method

2.3.1 Derivation logic and general formula

The derivation method for total wind and solar capacity used in this paper is driven jointly by the NDC emission constraints and the electricity supply–demand framework: starting from the NDC emission constraint and proceeding through sectoral emission-reduction responsibility decomposition and substitution-benefit estimation, the national net GHG emission constraint is translated into a lower bound for the electricity that must substitute for retired coal-fired generation; then, within the target-year electricity supply–demand framework, the total generation to be undertaken by wind and solar is determined jointly by the incremental electricity demand and the coal-generation retirement substitution; finally, combined with the NDC capacity policy target and regulation-margin considerations, an elastic installed-capacity interval adapted to different strategic orientations is determined.

The core assumption is equal substitution—that is, the additional electricity generated by wind and solar fully replaces the reduction in coal-fired generation, without considering system regulation losses. Its reasonableness lies in the following: with declining energy-storage costs and improved grid flexibility, system regulation losses are expected to be kept within a small range (<<5%) by 2035. This expectation is supported by the rapid deployment of utility-scale storage and the continuous enhancement of grid flexibility through inter-provincial coordination and demand-side response toward 2035. Meanwhile, the coal-generation retirement substitution converted under the equal-substitution assumption is a conservative lower bound, and the actual installed capacity should reserve an additional regulation margin on this basis, giving the calculation result a "bottom-line reference" value. If system regulation losses were higher, the effective generation per unit of installed capacity would be lower, and meeting the same emission and energy targets would require a larger installed capacity; the equal-substitution result therefore provides a conservative lower reference, and the interval upper bound should be interpreted with this margin in mind.

The general formula for total wind and solar capacity is

$$C = \frac{G_0 + G_{\text{sub}} + (D_t - D_0) - \Delta G_0}{\bar{h}} \tag{1}$$

where C is the total wind and solar installed capacity, G_0 is the base-year wind-and-solar generation, G_{sub} is the coal-generation retirement substitution, whose lower bound is determined by the NDC emission constraints (see Step 5), D_t and D_0 are the total electricity consumption in the target year and the base year, respectively, ΔG_0 is the increment of other generation sources (hydro, nuclear, gas, etc.) in the target year relative to the base year, and $\bar{h}$ is the weighted average utilization hours. Peak emissions P, the NDC emission reduction rate α, the share borne by the power sector λ, and the carbon emission intensity of coal-fired power β are defined in Steps 1–4.

2.3.2 Step-by-step derivation principle

Step 1: Determination of peak emissions. Synthesizing domestic and international research results, determine the national GHG peak emissions P and the peaking year.

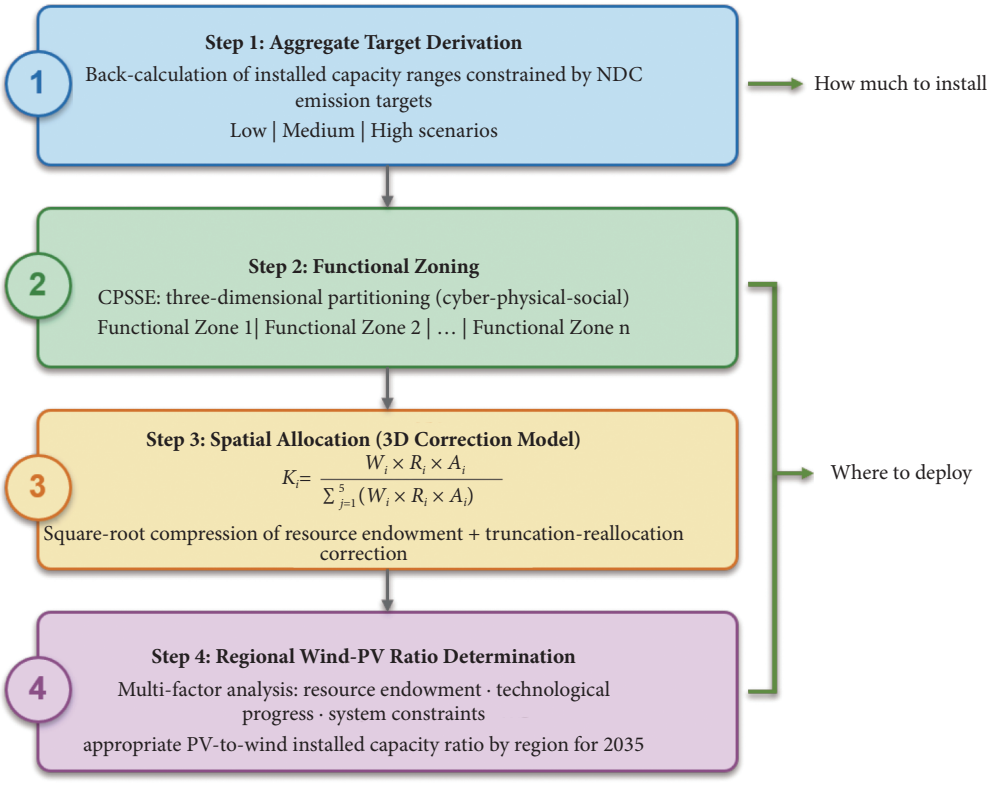


Fig. 1 Quantitative analysis workflow of total installed capacity and spatial distribution.

Step 2: Calculation of economy-wide emission reductions. Based on the NDC emission reduction rate α, calculate the absolute emission reduction $\Delta E = P \times \alpha$, and set low, medium, and high scenarios.

Step 3: Decomposition of power-sector emission-reduction responsibility. Let the share borne by the power sector be λ (slightly higher than its emission share, because decarbonization technologies are relatively mature); the emission reduction required of the power sector is $\Delta E_{\text{power}} = \Delta E \times \lambda$.

Step 4: Estimation of the substitution benefit of coal-power reduction. The carbon emission intensity of coal-fired power in the operating phase is denoted β; wind and solar generation are zero-carbon, so the unit substitution benefit is β.

Scope note: this paper adopts the operating-phase emission accounting scope. The life-cycle indirect emissions of wind and solar equipment manufacturing (approximately 10–50 g CO_2eq/(kWh))[21] amount to only 1.2%–6% of the operating emissions of coal-fired power[22], have a negligible effect on the derivation of total installed capacity, and are implicitly offset against the equipment-manufacturing emissions of coal-fired power, so they are not double-counted. This scope is consistent with the industry practice of institutions such as the International Energy Agency (IEA) and International Renewable Energy Agency (IRENA)[23,24].

Step 5: Estimation of the lower bound of coal-generation retirement substitution. Based on the power-sector emission reductions and the unit substitution benefit, and under the equal-substitution assumption, convert the power-sector emission-reduction responsibility into the lower bound of coal-generation retirement substitution required to satisfy the NDC emission constraints:

$$G_{\text{sub}}^{\min} = \frac{P \times \alpha \times \lambda}{\beta} \tag{2}$$

Step 6: Electricity supply–demand accounting and emission-coverage check. Within the target-year electricity supply–demand framework, carry out an electricity-balance accounting: project total electricity demand based on GDP growth and electrification-rate improvement; subtract the generation of coal power (with the retirement ratio set no lower than the lower bound in Eq. (2)), hydro, nuclear, gas, and other sources to obtain the total generation to be undertaken by wind and solar G; meanwhile, using the lower bound in Eq. (2) as the benchmark, verify the extent to which the emission reductions corresponding to the retired coal generation cover the power-sector emission-reduction responsibility; if the coverage is insufficient or the balance deviation is large, trace back and check the retirement ratio and parameter assumptions.

Step 7: Calculation of total installed capacity. Convert the wind-and-solar total generation determined in the supply–demand accounting into total installed capacity:

$$C = \frac{G}{\overline{h}} \tag{3}$$

The weighted average utilization hours $\overline{h}$ reflect the technology progress trend and capacity-mix optimization in the target year:

$$\overline{h} = \sum (h_k \times w_k) + \Delta h_{\text{tech}} \tag{4}$$

where h_k is the utilization hours of the k-th type of generation, w_k is the corresponding capacity share, and Δh_{tech} is the technology-progress gain.

2.3.3 Multi-constraint verification and robustness analysis of the installed-capacity interval

After the total installed capacity is determined, constraint verification is carried out from three aspects: resource potential, potential integration space, and industrial support. In terms of

resource potential, whether the national technically developable potential of wind and solar can support this capacity scale should be assessed. In terms of potential integration space, the acceptance limits of the target-year grid transmission capacity, storage configuration, and demand-response resources should be evaluated. In terms of industrial support, whether the production capacity of the PV module and wind-turbine industry chains can guarantee the average annual newly added capacity should be verified. Combining the above verification results, a reasonable installed-capacity interval that balances development and security can be determined; its elastic feature is reflected in the following: the lower bound corresponds to a steady development scenario, the upper bound to an accelerated-leapfrog scenario, and the median to an active and orderly scenario. Furthermore, sensitivity analysis of key parameters such as peak emissions P, the share borne by the power sector λ, the carbon emission intensity of coal power β, the weighted average utilization hours $\overline{h}$, and the average annual growth rate of electricity demand can be used to test the robustness of the installed-capacity interval.

2.4 Regional division method

2.4.1 Multi-dimensional basis for regional division

Traditional zoning methods are mostly oriented toward resource endowment or geographic macro-regions and insufficiently consider the coupling of physical and social systems. Within the CPSSE framework, this paper focuses on the interaction of the physical and social dimensions to construct the regional division criteria.

In the physical dimension, wind and solar resource endowment, grid transmission capacity boundaries, and electricity load distribution should be assessed to clarify whether each region can physically accommodate large-scale capacity and transmission requirements; among these, electricity load distribution is affected by national industrial-layout policies and should be reflected in the physical-constraint assessment. In the social dimension, economic and social development trends, national regional development strategies, and energy security goals should be incorporated to identify the functional positioning of each region in the national energy transition pattern.

2.4.2 Steps of functional regional division

Regional division proceeds as follows. First, from the social dimension, identify regions with national-level special strategic positioning as the core reference for zoning. Second, from the physical dimension, assess the matching relationship between resource endowment and grid transmission capacity in each region to clarify its relative position in the resource–grid pattern. Third, from the physical dimension, check the impact of national industrial-layout policies on regional electricity demand and renewable energy integration. Finally, integrate the above analysis to determine the core functional positioning of each region and delineate boundaries using provincial administrative units as the basic units. As national strategy evolves and technology breakthroughs and grid-structure changes occur, the functional positioning and boundaries of regions can be adjusted accordingly.

This method does not presuppose a fixed number of regions or a fixed hierarchy; the zoning resolution and the weights at each level can be flexibly adjusted according to research needs, and the method can be directly adapted to the analytical needs under different strategic orientations.

2.5 Three-dimensional correction model

2.5.1 Model construction and basis for coefficient selection

After the regional division and the aggregate target are determined, the national total wind and solar capacity needs to be decomposed among regions. This paper constructs a "strategic weight–resource endowment–integration capacity" three-dimensional correction model, and the allocation coefficient is calculated as Eq. (5):

$$K_i = \frac{W_i \times R_i \times A_i}{\sum_{j=1}^{5} (W_i \times R_i \times A_i)} \tag{5}$$

where K_i is the normalized allocation coefficient of region i; W_i is the strategic weight coefficient; R_i is the resource endowment coefficient; A_i is the integration capacity coefficient; and n is the number of functional regions. The three coefficients adopt a multiplicative form, and the underlying mechanism is that any region must simultaneously satisfy the three conditions of strategic priority, sufficient resources, and feasible integration to obtain a higher allocation coefficient. If a region has excellent resource endowment but insufficient potential integration space or low strategic priority, its allocation coefficient will still be suppressed.

The basis for coefficient selection is as follows: the strategic weight coefficient incorporates the priority of national energy security and transition strategy into the allocation process, ensuring that the distribution results are consistent with policy orientation; the resource endowment coefficient uses the technically developable potential as the measure, constraining the allocation results not to exceed the resource-carrying upper limit; and the integration capacity coefficient uses the load increment as the measure, constraining the allocation results not to exceed the grid acceptance capability.

2.5.2 Coefficient normalization method

R_i and A_i are normalized based on objective data, taking the nationally optimal region as the benchmark (with a value of 1) and assigning values to other regions by relative proportion; W_i is assigned by decision-makers according to the strategic orientation and satisfies the normalization constraint $\sum W_i = 1$.

(1) Resource endowment coefficient.

R_i reflects the ratio of the remaining technically developable wind and solar potential of each region to the nationally optimal level, with a value range of (0, 1]. Because the marginal cost of large-scale wind and solar development increases and ecological constraints tighten, linear normalization causes extreme resource-rich regions to be disproportionately amplified in the multiplicative model. A power-function compression $R_i' = R_i^{\gamma}$ (with $\gamma = 0.5$) is adopted to characterize the nonlinear conversion difficulty; this treatment draws on the idea of power transformation in statistics for compressing the dispersion of extreme values and is applied in an adaptive manner to the allocation imbalance caused by the extreme dispersion of resource endowment in this paper. Sensitivity tests (see Section 3.6.3) show that $\gamma = 0.5$ can effectively alleviate over-concentration of allocation while preserving regional resource differences.

$$R_i = \sqrt{\frac{D_i}{D_{i,\max}}} \tag{6}$$

where D_i is the remaining technically developable wind and solar potential of region i, and $D_{i,\max}$ is the maximum remaining technically developable potential among regions.

(2) Integration capacity coefficient

A_i uses the maximum load increment as the measure to characterize the renewable energy integration space formed by the growth of electricity demand in each region in the target year, with a value range of (0, 1]. The larger the regional electricity demand growth, the more abundant the potential integration space for new generation capacity.

$$A_i = \frac{\Delta L_i}{\Delta L_{i,\max}} \tag{7}$$

where ΔL_i is the maximum load increment of region i, and $\Delta L_{i,\max}$ is the maximum load increment among regions.

(3) Strategic weight coefficient

W_i reflects the relative priority of each region in national energy security, economic layout, and transition strategy. Unlike R_i and A_i, which are based on objective data, W_i reflects policy preferences and needs to be determined by integrating policy documents and scenario needs. Table 1 gives the weight-allocation principles under five typical strategic orientations.

In specific assignment, first determine the dominant strategic orientation according to the policy scenario, identify the core strategic regions and assign the highest weights (e.g., 0.30–0.40); regions performing important supporting functions are assigned medium weights (e.g., 0.20–0.25); and other regions are assigned lower weights according to their strategic positioning (e.g., 0.10–0.15), satisfying $\sum W_i = 1$. After completion, a reasonableness check is carried out: for example, under the resource-priority orientation, the Northwest region should have the highest weight, and under the local-balance orientation, the Eastern Coastal region should have the highest weight; if this expectation is not met, adjustments should be re-made.

2.5.3 *Engineering feasibility constraint correction*

The allocation coefficient obtained from Eq. (5) reflects the theoretical allocation result under ideal conditions. In actual planning, it is necessary to introduce a regional annual net-increment upper limit $\overline{\Delta}_i$ to check the theoretical value against engineering feasibility; when the theoretical allocation exceeds the region's actual engineering implementation capability, the truncation-and-redistribution algorithm is used to correct it. This upper limit is jointly constrained by factors such as land ecological carrying capacity, transmission-channel capacity, grid flexible dispatch and balancing-adjustment capability, industry-chain production capacity, and construction-organization conditions, reflecting the hard restrictions of multiple physical, information, and social conditions on planning implementation. This correction mechanism does not change the core model structure but is embedded as an external constraint layer, ensuring that the allocation results are practically implementable from an engineering perspective.

Let the theoretical allocation of region i be $\Delta C_i^{(0)} = K_i \times \Delta C_{\text{total}}$; the truncation-and-redistribution algorithm is as follows:

Step 1: $\Delta C_i^{(1)} = \min\left(\Delta C_i^{(0)}, \overline{\Delta}_i\right)$, and record the overflow amount $\Omega_i = \max\left(0, \Delta C_i^{(0)} - \overline{\Delta}_i\right)$;

Step 2: The total overflow amount $\Omega = \sum \Omega_i$ is redistributed according to the relative K_j proportions of the regions that have not reached their upper limits, that is, $\Delta C_j^{(2)} = \Delta C_j^{(1)} + \Omega \times \frac{K_j}{\sum_{m \in M} K_m}$, where $M = \left\{ m | \Delta C_m^{(0)} < \overline{\Delta}_m \right\}$;

Step 3: If new upper-limit violations are generated, repeat Steps 1 and 2 until all regions satisfy the upper-limit constraints.

The model has adjustment flexibility in terms of the number of regions, strategic orientations, and aggregate targets and can thereby generate distribution plans adapted to different policy scenarios without restructuring the core structure.

2.6 Method for determining the regional wind–solar ratio

After the aggregate allocation is completed, the PV-to-wind capacity ratio of each region needs to be further determined. This paper proposes a ratio-determination method that integrates resource conditions, technology progress trends, and system operation constraints.

2.6.1 *Multi-factor analysis framework*

This method carries out the analysis from the following three levels:

(1) Resource endowment assessment. The differences in wind and solar resources among regions constitute the basic basis for the ratio and need to be further analyzed in combination with the differences between PV and wind in output characteristics and land/sea occupation.

(2) Technology progress correction. Changes in the maturity of factors such as energy-storage costs, far-offshore wind technology, and the carrying capacity of distributed PV distribution networks affect the relative advantages of PV and wind in each region.

(3) System constraint verification. The grid structure, load characteristics, and regulating-resource configuration of each region jointly determine the potential integration space of renewables; the conditions for smoothing midday peaking, valley-load matching, and combined wind–solar output fluctuation need to be verified.

2.6.2 *Steps for designing the target-year wind–solar ratio*

Based on the above analysis, the PV-to-wind capacity ratio of each region in 2035 is determined according to the following steps:

(1) Basic direction determination. Determine the basic direction of the wind–solar ratio according to regional resource characteristics; for example, regions with superior offshore wind resources should increase the wind share, and regions with superior distributed-development conditions should increase the PV share.

(2) Technology progress correction. Correct the basic direction according to the technology maturity in the target year; raise the

Table 1 General principles for determining W_i (reusable for different strategic orientations).

Strategic orientation type	Weight allocation principle
Resource-priority	Assign high weights to resource-rich regions, highlighting resource-richness priority
Local-balance	Assign high weights to load-center regions, highlighting local self-sufficiency priority
Security-priority	Assign high weights to regions with improved local self-sufficiency, highlighting energy security autonomy
Economic-priority	Assign high weights to regions with the lowest wind and solar costs, highlighting cost optimality
Comprehensive-balance	Weighted average across dimensions, avoiding excessive concentration of a single orientation

share of technologies whose costs have declined significantly, and lower the share of technologies whose maturity lags or has limited room for improvement.

(3) System constraint verification. Incorporate the corrected ratio into the regional grid constraints for verification, ensuring that the midday PV output peak, nighttime wind output, and combined wind–solar fluctuation are all within the system's flattening capability.

(4) Determination of the target-year ratio. Integrate the above analysis to determine the PV-to-wind capacity ratio of each region in 2035, reflecting the wind–solar structure characteristics under long-term technology conditions.

3 Case application: total capacity and spatial distribution of wind and solar power in China in 2035

3.1 Data sources

The data used in this paper are mainly drawn from the following sources: the 2024 provincial wind-and-solar installed capacity data come from the annual electricity statistics published by the National Energy Administration; the wind-and-solar technically developable potential data come from the wind and solar energy resource assessment results of the National Climate Center of the China Meteorological Administration[25]; the 2024 provincial hourly electricity load data use the Chinese provincial electricity load curve dataset reconstructed based on meteorological variables by Yi et al.[26], and the 2035 load data are extrapolated and projected based on historical evolution trends; and the regional development strategic positioning refers to national planning documents such as the 14th Five-Year Plan for Renewable Energy Development and the National Plan on Major Function Zones.

3.2 Aggregate target: deriving the installed-capacity interval from NDC emission constraints

3.2.1 Parameter setting and emission-reduction scenarios

Referring to the estimation results of institutions such as Beijing Institute of Technology[27], the University of Chinese Academy of Sciences[28], and the IEA[29], China's GHG emissions peak at approximately 12–13 Gt CO_2eq; this paper takes peak emissions P = 12.6 Gt CO_2eq as the derivation benchmark. In 2024, the power sector accounted for approximately 45% of China's total emissions and has a relatively mature decarbonization technology pathway; therefore, it is set to bear 55% of the economy-wide emission-reduction task. The unit substitution benefit is β = 0.83 kg CO_2/(kWh), corresponding to the average operating carbon emission intensity of China's existing coal-fired units[30]. The NDC target requires economy-wide net GHG emissions in 2035 to decrease by 7%–10% relative to the peak; low, medium, and high emission-reduction scenarios are accordingly set, and the emission reductions and the lower bound of coal-generation retirement substitution under each scenario are shown in Table 2.

3.2.2 Electricity supply–demand accounting

The coal-retirement and generation-mix structure is placed in the 2035 electricity supply–demand framework for electricity-balance accounting. In terms of electricity demand, total electricity consumption in 2024 was approximately 9,850 TWh; considering economic growth and electrification-rate improvement, electricity demand in 2035 is projected at 15,100–15,900 TWh (the medium scenario takes the midpoint of 15,500 TWh). In terms of coal-fired generation, it was approximately 5,500 TWh in 2024; the coal-power retirement ratio is set no lower than the lower bound in Table 2 (11%–15%), while also accounting for natural unit retirement and deep substitution driven by electrification: in the low scenario, generation is approximately 4,700 TWh after 15% retirement; in the medium scenario, approximately 4,300 TWh after 22.5% retirement; and in the high scenario, approximately 3,900 TWh after 30% retirement. In terms of other sources, the combined generation of hydro and nuclear is expected to grow steadily to approximately 3,400 TWh, and gas-fired generation to approximately 500 TWh. The electricity-balance accounting and emission-constraint check results are shown in Table 3.

The accounting and check results show that, in all scenarios, the emission reductions corresponding to the retired coal generation (0.66–1.33 Gt) cover the power-sector emission-reduction responsibility (0.485–0.693 Gt), with a coverage ratio of approximately 1.4–1.9 times; the NDC emission constraint is satisfied at the power-sector level with a margin that widens as the reduction intensity increases. The total generation to be undertaken by wind and solar in 2035 under the supply–demand framework is 6,500, 7,300, and 8,100 TWh in the low, medium, and high scenarios, respectively, which is used as the input for the total installed-capacity calculation.

Table 2 NDC emission-reduction scenarios and the lower bound of coal-generation retirement substitution.

Scenario	Reduction rate	Economy-wide reductions (Gt)	Power-sector reductions (Gt)	Lower bound of coal-generation retirement substitution (TWh, share of 2024 coal generation)
Low	7%	0.882	0.485	584 (11%)
Medium	8.5%	1.071	0.589	710 (13%)
High	10%	1.260	0.693	835 (15%)

Table 3 Electricity-balance accounting within the electricity supply–demand framework and emission-constraint check.

Scenario	Total demand (TWh)	Coal generation (TWh)	Hydro + nuclear generation (TWh)	Gas generation (TWh)	Wind/solar generation required (TWh)	Emission reduction from coal retirement (Gt)	power-sector reduction responsibility (Gt)
Low (7%, 15% retirement)	15,100	4,700	3,400	500	6,500	0.66	0.485
Medium (8.5%, 22.5% retirement)	15,500	4,300	3,400	500	7,300	1.00	0.589
High (10%, 30% retirement)	15,900	3,900	3,400	500	8,100	1.33	0.693

3.2.3 Setting of weighted average utilization hours and calculation of total installed capacity

Considering the technology progress and capacity-mix optimization trend of wind and solar in 2035, the weighted average utilization hours are set at 1,720 h, and the calculation process is shown in Table 4.

The above settings are based on the following judgments: the wind capacity share increases to 45% in 2035 (with higher utilization hours of offshore wind and large-scale onshore wind turbines), and the PV share is 55% (with an optimized distributed and centralized layout). The 15 h technology-progress gain reflects the combined efficiency improvement brought by larger wind turbines, bifacial modules, and the widespread use of tracking mounts. This value is about 4%–7.5% higher than the current level (approximately 1,600–1,650 h), which is basically consistent with the expected trend of wind-and-solar technology iteration during the 15th and 16th Five-Year Plan periods. Based on the accounting-based wind-and-solar generation and the weighted average utilization hours, the installed capacity corresponding to the low, medium, and high scenario generation is 3,780, 4,240, and 4,710 GW, respectively. On this basis, the elastic installed-capacity interval is determined as follows: the lower bound is anchored to the NDC capacity policy target of 3,600 GW (wind and solar reaching more than six times the 2020 level); being lower than the low-scenario estimate, it indicates that the policy target is compatible with the electricity balance and leans toward prudence. The medium value takes the medium-scenario estimate of 4,200 GW. Considering that the equal-substitution assumption does not account for system regulation losses and that actual capacity needs to reserve a regulation margin, the upper bound is rounded up from the high-scenario estimate to 4,800 GW. Taking the existing installed capacity of 1,407 GW in 2024 as the base, the cumulative net increment from 2025 to 2035 is 2,193–3,393 GW, with an average annual net increment of 200–310 GW.

The 3,600–4,800 GW elastic interval as a whole covers the supply–demand framework estimation results and is mutually corroborated with the NDC capacity policy target. Further multi-constraint verification is carried out: in terms of resource potential, China's technically developable wind-and-solar potential is approximately 56,550 GW, and the target value accounts for only 6.4%–8.5%, so the resource constraint does not constitute a rigid limit; in terms of potential integration space, the Northwest region has a small local load and its existing transmission-channel utilization is nearly saturated, while the load centers in the East and Central regions have larger potential integration space but limited local resources; in terms of industrial support, the current annual PV module production capacity is approximately 500 GW, which can accommodate the implied PV additions of 110–170 GW per year; the current annual wind-turbine production capacity is approximately 80 GW, below the implied wind additions of 90–140 GW per year, so wind-turbine capacity would need to expand, especially in the high scenario. Combining the above constraints, a wind-and-solar scale of 3,600–4,800 GW in 2035 is a reasonable interval that balances development and security.

3.3 Regional division: delineation of five functional regions

From the physical dimension, the Northwest region has vast wind and solar resources but its transmission channels are approaching saturation; the Eastern Coastal region has huge offshore wind development potential and dense electricity load; the Southwest region has excellent wind and solar resources but high ecological sensitivity; and the Central-East Inland region has dense electricity load, scarce primary energy resources, and significant electricity demand growth. From the social dimension, the key provinces for clustered offshore wind development in the 14th Five-Year Plan, the "West-to-East power transmission" strategic corridors, major regional coordinated development strategies, and national industrial-layout policies such as "East Data, West Computing" constitute the core references for regional division by reshaping the spatial distribution of electricity demand and regional functional positioning. Integrating the above factors, China is divided into five functional regions, as shown in Table 5.

3.4 Spatial allocation: application of the three-dimensional correction model

3.4.1 Calculation of normalized allocation coefficients

Based on Eq. (5), the normalized allocation coefficient K_i of each region is obtained by normalizing the product of the resource endowment coefficient R_i, the integration capacity coefficient A_i, and the strategic weight coefficient W_i. Among them, R_i and A_i are calibrated by objective data, while W_i reflects the difference in strategic orientation and is the key lever for generating differentiated distribution plans. This paper designs two strategic scenarios to test the model's sensitive response to strategic orientation. Scenario A (West-to-East transmission dominated) continues the traditional transmission pattern, setting the strategic weight of the Northwest region at 0.35 (the highest) and that of the Eastern Coastal region at 0.20. Scenario B (local balancing dominated) focuses on local self-sufficiency in the East, raising the strategic weight of the Eastern Coastal region to 0.30 and lowering that of the Northwest region to 0.25. Among them, Scenario A corresponds to the "from afar" orientation (centralized development with inter-regional transmission), and Scenario B corresponds to the "from nearby" orientation (local development with local integration); together they reflect the two basic orientations of the strategic idea of combining "from afar" and "from nearby" mentioned in the Introduction. Scenario A reflects the long-standing "West-to-East power transmission" strategy embodied in national plans for large clean-energy bases and ultra high voltage (UHV) transmission corridors, whereas Scenario B reflects the recent policy emphasis on local integration and

Table 4 Weighted average utilization hours of wind and solar in 2035.

Generation type	Average utilization hours	Capacity share	Weighted contribution (h)
Wind	2,200 h (onshore 2,000 h, offshore 3,500 h)	45%	990
PV	1,300 h (distributed 1,100 h, centralized 1,500 h)	55%	715
Technology-progress gain	—	—	+15
Weighted average	—	100%	$\bar{h}$ = 1,720

Table 5 Division and positioning of the five functional regions.

Region	Provinces covered	Regional characteristics and strategic function	Development model
Northwest	Xinjiang; Qinghai; Gansu; Ningxia; Inner Mongolia	Abundant wind and solar resources and vast territory; the ballast stone of national energy security and the main force of West-to-East power transmission	Centralized wind-and-solar bases, UHV transmission
Eastern Coastal	Liaoning; Shandong; Jiangsu; Zhejiang; Fujian; Guangdong; Guangxi; Hainan	Electricity load among the highest nationwide; superior conditions for offshore wind and distributed PV; serving both as a receiving end and as a local generation base; an engine of the marine economy and a coastal green energy base	Large-scale offshore wind development, distributed PV
Southwest	Sichuan; Yunnan; Tibet; Chongqing; Guizhou	Outstanding hydropower regulation capability; good mountain wind and PV resources; high ecological sensitivity; a demonstration base for multi-energy complementarity and the second corridor of West-to-East power transmission	Hydro–wind–solar integrated bases
Central-East Inland	Beijing–Tianjin–Hebei; Yangtze River Delta (Shanghai, Anhui); Central China (Henan, Hubei, Hunan, Jiangxi)	Dense electricity load, scarce primary energy resources, and clustering of computing hubs; the core area of power supply security and a pilot zone of computing–electricity coordination	Distributed, demand response, computing–electricity coordination
Other	Heilongjiang; Jilin; Shanxi; Shaanxi, etc.	Diverse resource endowment and locational conditions, with multi-faceted development potential; regions developing according to local conditions	Both centralized and distributed development

distributed renewable development. Together they capture the two poles of the ongoing policy debate on accommodating 3,600 GW of wind and solar. The weights of the other regions are kept consistent in both scenarios. The comparison of the normalized allocation coefficients of each region under the two scenarios is shown in Figure 2.

The results show that the allocation coefficients of the Northwest region and the Eastern Coastal region reverse under the two strategic orientations: under Scenario A, the Northwest region dominates with an allocation coefficient of 0.49; under Scenario B, the Eastern Coastal region becomes the largest contributor of increments with a coefficient of 0.41. This indicates that the three-dimensional correction model can effectively identify the nonlinear impact of strategic-weight adjustment on the spatial allocation structure.

3.4.2 *Total allocation under the medium scenario*

Taking the medium scenario (4,200 GW) as an example, China's wind-and-solar installed capacity stock in 2024 is 1,407 GW, and the cumulative net increment from 2025 to 2035 is 2,793 GW. The 2035 target total of each region is calculated as Eq. (8):

$$C_i^{2035} = C_i^{2024} + K_i \times \Delta C_{\text{total}} \tag{8}$$

where C_i^{2024} is the wind-and-solar capacity stock of region i in 2024, ΔC_{total} is the national net increment over the planning period, and the net increment borne by region i is $\Delta C_i = K_i \times \Delta C_{\text{total}}$. Table 6 presents the allocation results of the 2035 target total and net increment of each region under the two strategic orientations.

3.4.3 *Engineering feasibility constraint correction*

The theoretical allocation values in Table 6 are checked against engineering feasibility. The annual net-increment upper limit of each region comprehensively considers cross-domain constraints such as land ecological carrying capacity, transmission-channel capacity, grid flexible dispatch and balancing-adjustment capability, industry-chain production capacity, and construction-organization conditions.

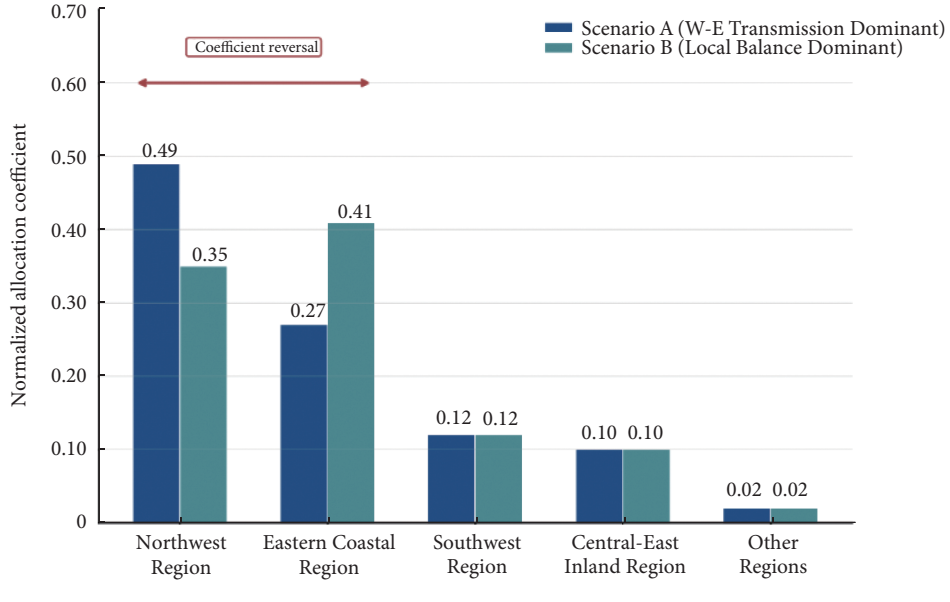


Fig. 2 Comparison of normalized allocation coefficients under two strategic orientations.

Table 6 Comparison of 2035 target totals under two strategic orientations in the medium scenario.

Region	Scenario A target total (GW)	Scenario A net increment (GW)	Scenario A net-increment share	Scenario B target total (GW)	Scenario B net increment (GW)	Scenario B net-increment share
Northwest	1,761	1,369	49.0%	1,374	982	35.2%
Eastern Coastal	1,156	759	27.2%	1,540	1,143	40.9%
Southwest	440	329	11.8%	441	330	11.8%
Central-East Inland	631	279	10.0%	632	280	10.0%
Other	213	58	2.1%	213	58	2.1%
Total	4,200	2,793	100.0%	4,200	2,793	100.0%

Northwest region: from the physical dimension, the total transmission capability of existing and under-construction ultra-high-voltage direct current (UHVDC) corridors by 2035 is approximately 850–1,000 GW; with a renewable share of 75%–80%, the space for transmitted renewable capacity is approximately 640–800 GW. In terms of local integration, the maximum load in 2035 is approximately 310 GW, and the local new integration space is approximately 120–250 GW. From the social dimension, after deducting the ecological red lines and the compatibility restrictions of PV-based desertification control, the actual developable area is reduced by approximately 15%–20%. Combining the above constraints, the net-increment upper limit of the Northwest region is taken as 1,100 GW (transmission 700 + local 200 + stock replacement 200, conservatively rounded).

Eastern Coastal region: from the physical dimension, the national 14th Five-Year Plan for Renewable Energy Development specifies five 10-GW-class offshore wind bases; superimposed on the far-offshore wind expansion plan, the planned total offshore wind installed capacity in 2035 is approximately 120–130 GW. From the perspective of the industry chain and construction conditions, the current annual construction capability of China's core offshore wind equipment is approximately 8–10 GW; considering far-offshore technology iteration and equipment expansion, the annual construction capability in 2035 can be increased to 12–15 GW, but constrained by the typhoon season and monsoon period, the construction window is approximately 6–8 months per year. On balance, the cumulative net-increment upper limit from 2025 to 2035 is approximately 1,050 GW.

The theoretical net increments of the remaining regions do not exceed their land ecological carrying capacity, distribution-network integration capacity, or local industry-chain support capability, so no truncation correction is triggered. After constraint correction, under Scenario A the Northwest net increment is 1,100 GW (39.4%), the Eastern Coastal region 901 GW (32.2%), the Southwest region 392 GW (14.0%), the Central-East Inland region 332 GW (11.9%), and other regions 69 GW (2.5%); under Scenario B, the Northwest region decreases to 1,037 GW (37.1%), the Eastern Coastal region increases to 1,050 GW (37.6%), the Southwest region 349 GW (12.5%), the Central-East Inland region 296 GW (10.6%), and other regions 61 GW (2.2%). The net increments of all regions under the two scenarios sum to 2,793 GW, corresponding to a total wind-and-solar capacity of 4,200 GW in 2035; the truncation-and-redistribution algorithm converges in one iteration, and the total overflow has been fully redistributed to the regions that have not reached their upper limits. The results show that, under both strategic orientations, the Northwest and Eastern Coastal regions shift from unconstrained theoretical growth to constrained finite growth; under the local-balancing orientation, the East and the Northwest form a coordinated growth pattern, revealing the rigid constraint of physical limits on strategic visions—even when the East is given the highest weight, its upper limit still prevents it from independently undertaking the largest increment without the Northwest. The comparison of net increments before and after constraint correction is shown in Figure 3.

3.5 Wind–solar ratio: regional wind–solar ratio in 2035

After the total installed capacity of each region is determined, the PV-to-wind capacity ratio needs to be comprehensively determined in combination with resource endowment,

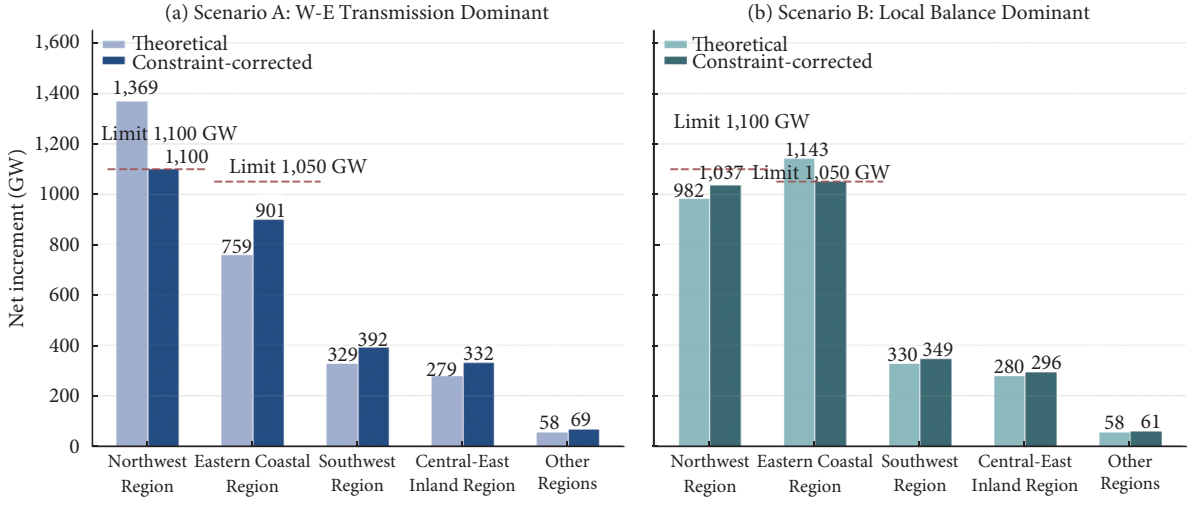


Fig. 3 Comparison of net increments before and after constraint correction in the medium scenario.

technology progress, and system operating conditions. Taking the Eastern Coastal region as an example: the region has high wind-energy density and long utilization hours, and its resource endowment naturally favors a high wind share (approximately 1:3); by 2035, the maturity of far-offshore wind technology will significantly reduce the levelized cost, further strengthening wind competitiveness (approximately 1:4); however, wind output fluctuation needs to be flattened by inter-provincial coordination and storage, and the share should not be too high to avoid raising system regulation costs (approximately 1:3.5). After comprehensive weighing, the wind–solar ratio of the Eastern Coastal region in 2035 is set at 1:3.5; other regions adopt the same analytical logic and are determined one by one. It should be noted that the ratio is determined through qualitative multi-factor judgment integrating resource endowment, technology progress, and system operating constraints, rather than through formal optimization; a rigorous optimization of the ratio would require system-level simulation and is left for future work. The 2035 PV-to-wind capacity ratio of each region is shown in Figure 4.

Based on the above ratios, the PV and wind installed capacity of each region is decomposed, and the national PV-to-wind capacity ratios under the two scenarios are both close to 1:1, basically consistent with the technology-progress assumptions in Table 4, with slight deviations arising from differences in the regional allocation structure. The specific composition of the 2035 wind-and-solar installed capacity of each region is shown in Figure 5.

3.6 Results and discussion

3.6.1 Policy implications of the aggregate target

The elastic interval of 3,600–4,800 GW corresponds to three policy orientations: 3,600 GW (low scenario) is a steady

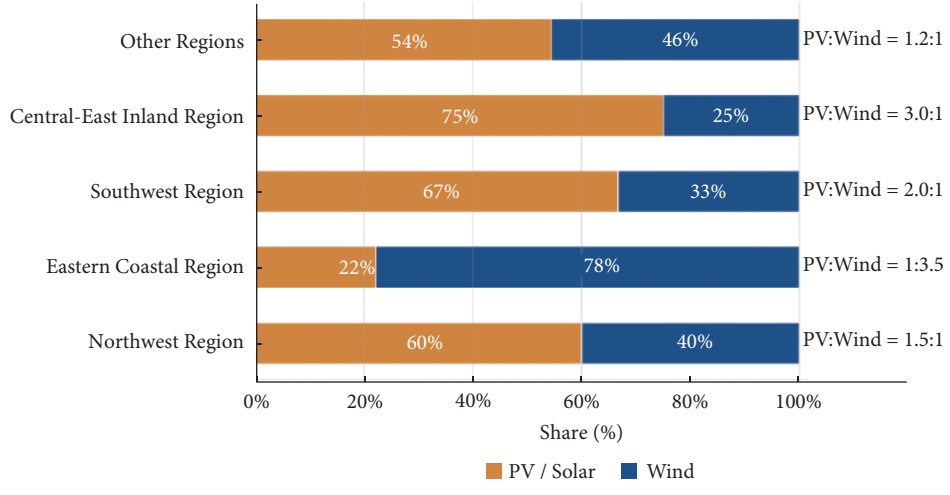


Fig. 4 PV-to-wind capacity ratio of each region in 2035.

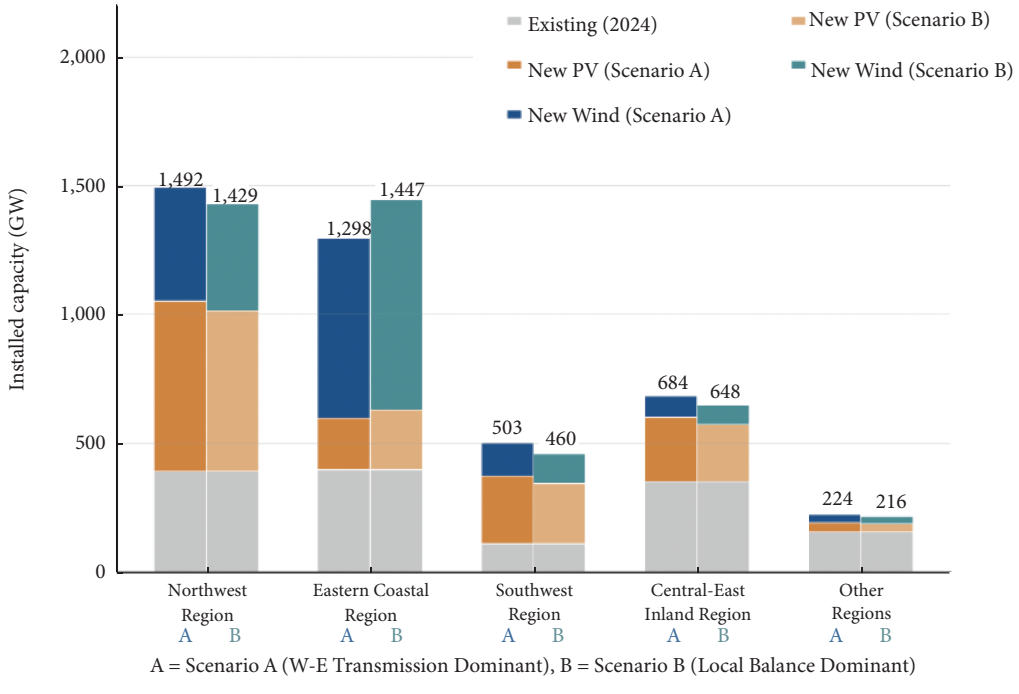


Fig. 5 Composition of 2035 wind-and-solar installed capacity under two strategic orientations in the medium scenario.

development pathway that emphasizes matching integration capability and is suitable for scenarios where grid infrastructure construction is relatively lagging; 4,200 GW (medium scenario) is an active and orderly pathway that balances development speed and system security and can serve as a baseline reference; and 4,800 GW (high scenario) is an accelerated-leapfrog pathway that serves national strategic needs and requires advanced configuration of transmission channels and storage facilities. This elastic interval enables decision-makers to make differentiated choices according to actual integration space, industrial capacity, and strategic orientation, avoiding the deficiency of a single rigid target. It should be noted that, after decomposition to the power sector, the NDC emission constraint requires only that coal-fired generation decline by approximately 11%–15% relative to 2024, constituting a non-binding constraint on total wind-and-solar installed capacity; the 3,600–4,800 GW installed-capacity scale is driven mainly by incremental electricity demand and the NDC capacity target, with the emission constraint functioning mainly to differentiate scenarios through the pace of coal retirement.

3.6.2 *Strategic sensitivity of spatial distribution*

After constraint correction, the spatial distribution reflects a dual response to strategic weights and physical constraints, showing three characteristics:

(1) The Northwest region: a basic support zone under physical upper-limit constraints. The net increments under Scenario A and Scenario B are 1,100 GW (39.4%) and 1,037 GW (37.1%), respectively, a difference of 63 GW, indicating that the upper limits of transmission channels and ecological constraints have substantially compressed the adjustment space of strategic weights, transforming the Northwest from a "strategically adjustable growth pole" into a "basic support zone rigidly constrained by physical boundaries".

(2) The Eastern Coastal region: the expansion side in the coordinated advancement pattern. The net increments under Scenario A and Scenario B are 901 GW (32.2%) and 1,050 GW (37.6%), respectively, making it the region with the largest adjustment in net increment after constraint correction. However, the sea-area and construction upper limit of 1,050 GW determines that it cannot fully replace the Northwest. Under Scenario B, the East (37.6%) and the Northwest (37.1%) form a coordinated advancement pattern.

(3) The remaining regions: the recipients of increment redistribution. The theoretical net increments of the Southwest, Central-East Inland, and other regions are close in value, but after constraint correction, Scenario A provides 43, 36, and 8 GW more than Scenario B, respectively. The spillover increments after the Northwest or the East reaches its upper limit are redistributed according to the proportions of the allocation coefficients of the regions that have not reached their upper limits, transforming the inland regions from passively configured objects into recipients of increment redistribution. The Southwest region gains 43 GW more in Scenario A than in Scenario B, indicating that when the Northwest transmission hits the constraint boundary, hydropower regulation capability becomes the preferred choice for undertaking the spillover increment.

3.6.3 *Robustness and validity verification of the method*

The sensitivity to strategic orientation is verified by the difference in allocation results between Scenario A and Scenario B: under Scenario A, the Northwest net-increment share is higher than that of the Eastern Coastal region; under Scenario B, the opposite pattern appears, and the ranking of the core regions is swapped under the two orientations. The truncation-and-redistribution algorithm converges in a single iteration (see Section 2.5.3), indicating that a moderate adjustment margin is reserved between the upper-limit setting of each region and the theoretical allocation.

Figure 6 shows that the installed-capacity interval is robust to reasonable fluctuations in key parameters: emission-side parameters such as peak emissions, the power-sector share, and the carbon emission intensity of coal power only change the lower bound of coal-generation retirement substitution, with an impact on the installed-capacity interval within ±20 GW; the interval fluctuates mainly with the weighted average utilization hours and the electricity demand growth rate, extending to approximately 3,540–4,860 GW under the extreme parameter combinations shown in Figure 6, while the core interval is maintained at 3,600–4,800 GW. Changes in the upper-limit parameters also affect the distribution structure: if the Northwest transmission capability unexpectedly increases to 1,200 GW, the allocation difference between Scenario A and Scenario B will correspondingly widen; if the East sea-area approval is tightened to 950 GW, the coordinated advancement pattern will shift toward a single Northwest-dominated pattern.

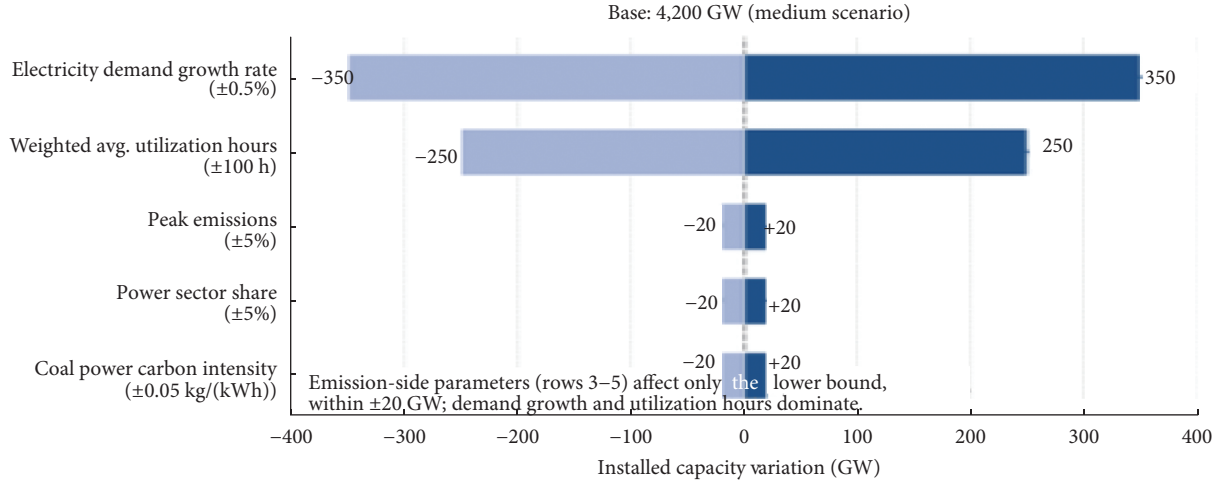


Fig. 6 Tornado chart of sensitivity analysis of key parameters.

From the comparison of the two strategic orientations, the constraint-correction results show that the Northwest and the East together constitute the main body of the net increment in the medium scenario (2,001 GW under Scenario A, accounting for 71.6%; 2,087 GW under Scenario B, accounting for 74.7%), forming a clear physical boundary. Specifically, even under the local-balancing orientation, the East still needs to rely on the Northwest for transmission; under the West-to-East transmission orientation, the East also needs to undertake at least 900 GW of local development tasks. This indicates that the coordinated advancement of the Northwest and the East is not determined solely by strategic orientation but is an objective result constrained by physical conditions.

The value of the resource-endowment compression parameter γ has an important influence on the allocation structure. This paper carries out a sensitivity comparison by setting γ = 0.3, 0.5, 0.7, and 1.0 to test the applicability of γ = 0.5, and the results are shown in Table 7.

The results show that γ = 1.0 (linear normalization) makes the Northwest share as high as 0.76 and 0.63 in Scenario A and Scenario B, respectively, while the Central-East Inland region is only 0.04, and the adjustment effect of strategic weights is masked by resource-endowment differences. γ = 0.3 over-compresses the resource differences: the Northwest share falls to 0.37 (Scenario A) and 0.25 (Scenario B), the Central-East Inland region rises to 0.13, and the resource discrimination is obviously weakened. γ = 0.7 provides insufficient compression: the Northwest share in Scenario A rebounds to 0.61, the Central-East Inland region falls to 0.07, and the allocation results again show a tendency toward over-concentration in the Northwest. In contrast, atγ = 0.5, the Northwest accounts for 0.49 (Scenario A) and 0.35 (Scenario B), and the Central-East Inland region for 0.10; the strategic differences are clear, and each region receives a significant non-zero share, achieving a balance between resource discrimination and allocation balance.

4 Conclusion

Within the CPSSE framework, this paper proposes a total-capacity and spatial-allocation method for wind and solar power that is suitable for different strategic orientations. By constructing a "strategic weight–resource endowment–integration capacity" three-dimensional correction model, the multiple constraints are incorporated into a quantifiable analytical framework; a square-root compression treatment of the resource endowment coefficient is introduced to alleviate the over-concentration of theoretical allocation under extremely dispersed resource endowment, and the truncation-and-redistribution correction mechanism is used to improve the engineering applicability of the model. The case application shows that: (1) driven jointly by the NDC emission constraints and the electricity supply–demand framework, the elastic interval of wind-and-solar installed capacity in 2035 is 3,600–4,800 GW; among them, the emission constraints are translated, through sectoral emission-reduction responsibility decomposition, into a lower bound of coal-generation retirement substitution, the supply–demand framework determines the scale of wind-and-solar generation, and the NDC capacity target anchors the lower bound of the interval—the three are mutually corroborated, and the interval is robust; (2) adjusting the strategic weights can generate differentiated distribution plans, and the allocation coefficients of the Northwest region and the Eastern Coastal region reverse under the West-to-East transmission and local-balancing orientations, indicating that the model is sensitive to changes in strategic orientation; and (3) after engineering feasibility constraint correction, both the Northwest and the East, the two core growth poles, are subject to physical upper limits, and under the local-balancing orientation the East and the Northwest form a coordinated advancement pattern rather than absolute East dominance, indicating that under high development intensity, engineering constraints impose rigid restrictions on strategic visions. For policymakers and energy planners, the proposed method offers an operational tool for translating national NDC capacity targets into regionally feasible deployment plans, balancing strategic orientation with physical constraints.

This study has the following limitations: (1) it focuses on the 2035 target year and does not address year-by-year implementation pathways; (2) the integration capacity coefficient is approximated by the load increment and does not incorporate grid operation details such as dynamic optimization of transmission-channel utilization; and (3) the aggregate derivation is based on the equal-substitution assumption and does not consider system regulation losses. Future research can be deepened in the following directions: first, carrying out year-by-year source–grid coordinated optimization to construct a transition mechanism from the target-year snapshot to the implementation pathway; second, incorporating the constraint-correction parameters into the dynamic updating of the integration capacity coefficient to improve the model's time-varying adaptability; and third, combining high-resolution climate data to assess the impact of spatiotemporal changes in wind and solar resources on the spatial distribution.

Appendix 1: detailed basis for regional division

(1) Jiangsu, Zhejiang, and Guangdong rank among the top nationwide in electricity load and possess high-quality offshore wind resources, serving both as electricity receiving ends and local generation bases; they are therefore assigned to the Eastern Coastal region. Shanghai has limited offshore wind capacity and prominent supply-security pressure, and together with Anhui forms the core of the Yangtze River Delta inland area; it is therefore assigned to the Central-East Inland region.

(2) Guangdong, Fujian, Zhejiang, Jiangsu, and Shandong are key provinces for clustered offshore wind development in the national 14th Five-Year Plan; Liaoning is the only coastal province in Northeast China and a strategic fulcrum for offshore wind development in the northeast; Guangxi and Hainan are core

Table 7 Sensitivity analysis of the resource-endowment compression parameter γ (medium scenario).

γ	Scenario A Northwest K_i	Scenario A Central-East Inland K_i	Scenario B Northwest K_i	Scenario B Central-East Inland K_i
0.3	0.37	0.13	0.25	0.13
0.5	0.49	0.10	0.35	0.10
0.7	0.61	0.07	0.46	0.08
1.0 (linear)	0.76	0.04	0.63	0.04

provinces of the Beibu Gulf offshore wind base (one of the five 10-GW-class offshore wind bases explicitly specified in the 14th Five-Year Plan for Renewable Energy Development); Guangdong, Guangxi, and Hainan constitute China's maritime gateway belt facing the Association of Southeast Asian Nations (ASEAN), a frontier for the docking of the Belt and Road Initiative with the ASEAN Connectivity Master Plan 2025.

(3) Although Chongqing and Guizhou have less hydropower than Sichuan and Yunnan, they have greater mountain wind potential; assigning them to the Southwest region can form a complementary pattern of "Sichuan–Yunnan–Xizang hydropower regulation + Chongqing–Guizhou mountain wind".

(4) The core characteristics of the Central-East Inland region are scarce primary energy resources and huge electricity demand. It mainly includes the Beijing–Tianjin–Hebei area, the Yangtze River Delta (Shanghai, Anhui), and the four Central China provinces (Henan, Hubei, Hunan, Jiangxi). Among them, the Beijing–Tianjin–Hebei area and the Yangtze River Delta correspond to the hub nodes of "East Data, West Computing", and the Central China region has dense electricity load and is a major receiving end of "West-to-East power transmission".

(5) The other regions refer to the remaining provinces without national-level special strategic positioning, which need to determine their own development pace according to their resource endowment and integration conditions.

Appendix 2: basis for determining the coefficients of the three-dimensional correction model

Table A1 Remaining technically developable wind-and-solar potential of each region (GW).

Region	2024 wind capacity	2024 PV capacity	2024 wind + solar total	Technically developable potential	Remaining technically developable potential
Northwest	199.06	192.98	392.04	41,516.00	41,123.96
Eastern Coastal	278.86	118.55	397.41	4,780.00	4,382.59
Southwest	75.05	36.03	111.08	4,761.00	4,649.92
Central-East Inland	250.75	101.22	351.97	2,812.00	2,460.03
Other	82.94	71.90	154.84	2,683.00	2,528.16

Table A2 Maximum load increment of each region (GW).

Region	2024 maximum load	2035 maximum load	Maximum load increment
Northwest	181.72	312.16	130.44
Eastern Coastal	685.81	1,073.35	387.54
Southwest	195.89	358.91	163.02
Central-East Inland	457.90	711.70	253.79
Other	124.15	201.85	77.70

Acknowledgements

This work is granted by the National Key R&D Program of China (2024YFF0809203).

Author contribution statement

Xueting Li is responsible for methodology and model design, formal analysis, investigation and data processing, visualization, writing of the original draft, and review and editing. Bin Cai is responsible for proposing the overall research objectives, supervision, methodology guidance, and review and editing. Yusheng Xue is responsible for supervision and the conceptualization of the cyber-physical-social system in energy (CPSSE) framework. Feng Xue is responsible for providing methodology guidance. Baoguo Shan, Qingchen Chao, Peipei You, and Yang Wang are responsible for providing research resources and data and for participating in the discussion of the research methodology. All the authors have approved the final manuscript.

Data availability

The data that support the findings of this study is available from the corresponding author upon reasonable request.

Use of AI statement

None.

Declaration of competing interest

Xueting Li, Bin Cai, Yusheng Xue, and Feng Xue are employees of State Grid Electrical Power Research Institute (NARI Group Corporation). Baoguo Shan and Peipei You are employees of State Grid Energy Research Institute Co., Ltd. The authors have no competing interests to declare that are relevant to the content of this article.

References

[1] IPCC. (2023). Climate Change 2023: Synthesis Report. Contribution of Working Groups I, II and III to the Sixth Assessment Report of the Intergovernmental Panel on Climate Change. Geneva: IPCC. https://doi.org/10.59327/IPCC/AR6-9789291691647.

[2] Zhou, Y., Han, J., Qu, Y., Collett, M., Grubb, M., Sharpe, S., Liu, Y. T., Huang, J. L., Zhang, D. (2026). Maintaining security of power supply in the context of technological change driven by low-carbon transition. *Energy and Climate Management*, 2(2): 9400033.

[3] IRENA. (2025). Renewable Capacity Statistics 2025. Abu Dhabi: International Renewable Energy Agency.

[4] Zhang, X. L., Huang, X. D., Zhang, D., Geng, Y., Tian, L. X., Fan, Y., Chen, W. Y. (2022). Research on the pathway and policies for

China's energy and economy transformation toward carbon neutrality. *Journal of Management World*, 38(1): 35–51.
[5] Cai, S. K. (2021). Challenges of dual-carbon goals and outlook for power structure adjustment trends. *Southern Energy Construction*, 8(3): 8–17.
[6] IEA. (2025). World Energy Outlook 2025. Paris: IEA Publications.
[7] Climate Change Center of China Meteorological Administration. (2025). Blue Book on Climate Change in China 2025. Beijing: Science Press. (In Chinese)
[8] Liu, J. C., Ma, X. Y., Lu, C. R. (2024). A three-stage framework for optimal site selection of hybrid offshore wind-photovoltaic-wave-hydrogen energy system: a case study of China. *Energy*, 313: 133723.
[9] Uguz, Y. F., Bilgili, A., Uzar, M. (2026). Toward improved siting of wind–solar hybrid farms: a novel framework integrating multi-criteria decision making, machine learning-driven feature selection, and spatial clustering. *Applied Energy*, 411: 127609.
[10] Lu, L., Wei, M. K., Zhang, H. Y., Jiang, L., Shen, L., Liao, K. (2024). Coordinated siting and sizing planning method of wind and photovoltaic power stations considering static voltage stability. *Electric Power Automation Equipment*, 44(1): 95–102.
[11] Zhou, B. X., Ning, C., Chen, S., Zhu, M., Su, Y. Q., Zhou, Y., Zang, T. L. (2024). Capacity planning and layout optimization method of wind and photovoltaic power plants in new energy base considering ecological resistance cost. *Electric Power Automation Equipment*, 44(7): 141–148.
[12] Kocabaldır, C., Yücel, M. A. (2023). GIS-based multicriteria decision analysis for spatial planning of solar photovoltaic power plants in Çanakkale province, Turkey. *Renewable Energy*, 212: 455–467.
[13] Noorollahi, Y., Senani, A. G., Fadaei, A., Simaee, M., Moltames, R. (2022). A framework for GIS-based site selection and technical potential evaluation of PV solar farm using Fuzzy-Boolean logic and AHP multi-criteria decision-making approach. *Renewable Energy*, 186: 89–104.
[14] Hashemizadeh, A., Ju, Y. B., Abadi, F. Z. B. (2024). Policy design for renewable energy development based on government support: a system dynamics model. *Applied Energy*, 376: 124331.
[15] Pourramezan, A., Samadi, M. (2023). A system dynamics investigation on the long-term impacts of demand response in generation investment planning incorporating renewables. *Renewable and Sustainable Energy Reviews*, 171: 113003.
[16] Hörsch, J., Brown, T. (2017). The role of spatial scale in joint optimisations of generation and transmission for European highly renewable scenarios. In Proceedings of the 2017 14th International Conference on the European Energy Market (EEM), Dresden, Germany, 1–7.
[17] Liu, J. Z., Wang, Q. H., Hu, Y., Fang, F. (2023). Connotation, characteristics and key technologies of new power systems. *New Type Power Systems*, 1(1): 49–65. (In Chinese)
[18] Liu, X. L., Cui, L. L., Ge, Q., Jiang, L. L., Jiang, Y., Li, B., Du, X. W. (2019). New ideas for the energy development strategy of central and eastern China. *China Population, Resources and Environment*, 29(6): 1–9.
[19] Shu, Y. B., Xue, Y. S., Cai, B., Han, J. G., Ling, W., Chen, X. Y., McElroy, M. B. (2018). A review of energy transition analysis part one elements and paradigms. *Automation of Electric Power Systems*, 42(9): 1–15.
[20] Xue, Y. S., Yu, X. H. (2017). Beyond smart grid—cyber–physical–social system in energy future [point of view]. *Proceedings of the IEEE*, 105(12): 2290–2292.
[21] IPCC. (2014). Climate Change 2014: Mitigation of Climate Change. Contribution of Working Group III to the Fifth Assessment Report of the Intergovernmental Panel on Climate Change. Cambridge: Cambridge University Press.
[22] UNECE. (2022). Carbon Neutrality in the UNECE Region: Integrated Life-cycle Assessment of Electricity Sources. Geneva: UNECE.
[23] IEA. (2025). Life Cycle Upstream Emissions Factors 2025. Paris: International Energy Agency.
[24] IRENA. (2024). Renewable Power Generation Costs in 2023. Abu Dhabi: International Renewable Energy Agency.
[25] Wang, Y., Chao, Q. C., Zhao, L., Chang, R. (2022). Assessment of wind and photovoltaic power potential in China. *Carbon Neutrality*, 1(1): 15.
[26] Yi, B. W., Luo, Q., Zhang, S. H., Ji, Y. L., Yu, S. M., Fan, Y. (2026). Hourly electricity load curve dataset for Chinese provinces derived from meteorological variables. *Scientific Data*, 13(1): 978.
[27] Wei, Y. M., Yu, B. Y., Tang, B. J., Liu, L. C., Liao, H., Chen, J. M., Sun, F. H., An, R. Y., Wu, Y., Tan, J. X., et al. (2022). Roadmap for achieving China's carbon peak and carbon neutrality pathway. *Journal of Beijing Institute of Technology (Social Sciences Edition)*, 24(4): 13–26.
[28] Zhang, L., Ruan, J. H., Zhang, Z., Qin, Z. Y., Lei, Z. Y., Cai, B. F., Wang, S. Y., Tang, L. (2024). City-level pathways to carbon peak and neutrality in China. *Cell Reports Sustainability*, 1(5): 100102.
[29] IEA. (2021). An Energy Sector Roadmap to Carbon Neutrality in China. Paris: International Energy Agency.
[30] China Electricity Council. (2025). Annual Development Report of China's Power Industry 2025. Beijing: China Electric Power Press. (In Chinese)



Xueting Li received her master's degree in technical economics and management from North China Electric Power University, Beijing, China, in 2023. She is currently a Junior Engineer at the State Grid Electric Power Research Institute (NARI Group Corporation), Nanjing, China. Her research focuses on medium- and long-term energy and power transition pathways, carbon peak and carbon neutrality strategy planning, and decision support for provincial power-source transitions.